

Exploration of Orally Available Calpain Inhibitors 2: Peptidyl Hemiacetal Derivatives

Yoshihisa Shirasaki,* Masayuki Nakamura, Masazumi Yamaguchi, Hiroyuki Miyashita,† Osamu Sakai, and Jun Inoue
 Senju Pharmaceutical Company, Ltd., 1-5-4 Murotani, Nishi-ku, Kobe, Hyogo 651-2241, Japan

Received February 11, 2006

We previously reported a potent calpain inhibitor **1** (SJA6017, *N*-(4-fluorophenyl)-*L*-valyl-*L*-leucinal), which displayed relatively low oral bioavailability (BA). Replacing the metabolically labile aldehyde moiety of **1** with more chemically stable warheads, such as a cyclic hemiacetal, hydrazone, and α -ketoamide, provided the inhibitors with improved in vitro metabolic stability. Cyclic hemiacetal **2** was the most stable of these compounds. The optimization of **2** led to hemiacetal **8** (SNJ-1715) which exhibited high potency, good aqueous solubility, excellent oral BA, and prolonged plasma half-life in rats. Furthermore, **8** showed neuroprotective efficacy via oral administration in a rat retinal ischemia model.

Introduction

Calpains, which are activated by calcium ions, are nonlysosomal cytosolic cysteine endoproteases, and several isoforms have been reported.¹ Two major isoforms, μ -calpain (calpain I) and *m*-calpain (calpain II), are ubiquitously found in mammalian cells. These enzymes are implicated in a variety of biological processes and in numerous diseases, such as muscular dystrophy, cardiac ischemia, cataract, stroke, Alzheimer's disease, central nervous system diseases, spinal cord injury, and traumatic brain injury (TBI).² Therefore, the development of novel agents that target calpains could potentially offer a means of treating these diseases.

Most calpain inhibitors consist of an active site (warhead) and a di or tripeptide-based backbone that is structurally related to the cleavage site of the substrates (Arg, Phe, Nle or Leu at the P1 site and Leu or Val at the P2 site).^{3–5} Calpain inhibitors are categorized into irreversible and reversible inhibitors by their mechanism of action.³ Irreversible inhibitors have an epoxide, α -haloketone, vinyl sulfone, or diazomethyl ketone moiety as warheads. These react with the SH group in the catalytic center of the enzymes and form irreversible covalent adducts.⁶ However, aldehydes, α -ketoesters, α -ketoacids, and α -ketoamides act as reversible warheads and form a hemithioacetal or ketal with the SH group.⁶ From the viewpoint of drug discovery, previous studies of calpain inhibitors have focused on reversible inhibitors because irreversible inhibitors may cause unexpected adverse effects. A number of reversible calpain inhibitors have been identified.³ Some, such as leupeptin,⁷ calpain inhibitor I,⁸ MDL 28170,⁹ AK295,¹⁰ A-705239,¹¹ and SJA6017 (**1**),¹² have shown neuroprotective efficacy in animal ischemia models.^{13–18}

Our group has previously reported that neuronal cell death occurs because of the activation of calpains in a rat retinal ischemia–reperfusion model. A potent calpain inhibitor, dipeptidyl aldehyde **1**, showed neuroprotective efficacy in this model when 3 mg/kg was administered intravenously.¹⁹ Thus, **1** may serve as a useful agent for the treatment of retinal neurological disorders such as glaucoma and retinitis pigmentosa. Because these retinal disorders are usually chronic diseases, the development of an oral drug is desirable because intravenous administration (iv) would be inconvenient. Instillation of an ophthalmic

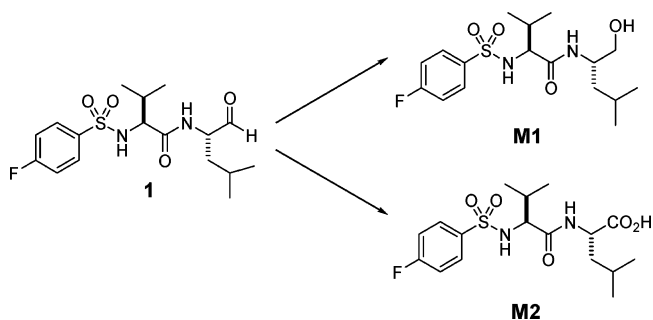


Figure 1. Main metabolic pathway of **1**.

solution in the eye cannot readily deliver drugs into the retina because several barriers lie between the retina and the surface area of the eye.²⁰ Oral administration of **1** showed efficacy in this model, but a relatively high dosage (500 mg/kg \times 2) is required.²¹ Hence, this phenomenon would limit its potential as a therapeutic agent for these diseases.

A pharmacokinetic (PK) study of **1** revealed that it showed poor bioavailability and very high total clearance in rats. We have reported that **1** possesses moderate Caco-2 membrane permeability, whereas both its in vitro metabolic stability against the human liver S9 fraction (S9) and its water solubility are low.²² Because aldehyde **1** is rapidly metabolized to the corresponding alcohol M1 and carboxylic acid M2 in human S9 in vitro and rats in vivo (Figure 1), the aldehyde moiety was a major metabolic soft spot. Assuming that metabolism is the major route of clearance, the conversion of the aldehyde moiety into more chemically stable warheads could lead to the generation of compounds with improved pharmacokinetics.

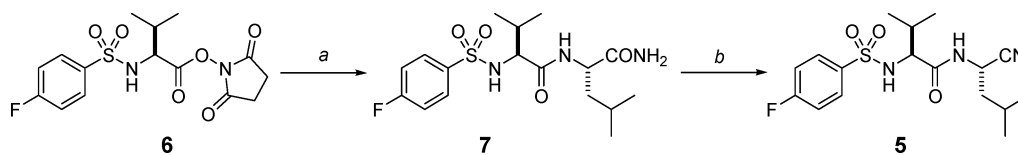
In this article, we describe the design and synthesis of novel compounds based on the modifications of the metabolic soft spot of **1** into various alternative warheads and describe further optimization studies to maximize potency. This article also reports the results of pharmacokinetic studies and the neuroprotective efficacy of a representative compound in the retinal ischemia model in rats.

Chemistry

We have reported the synthesis of hemiacetal **2**,²³ hydrazone derivative **3**,^{22a} and ketoamide **4**.²³ As shown in Scheme 1, nitrile **5** was synthesized from condensation of *N*-(4-fluorophenyl)-*L*-valine succinimide ester (**6**) and *L*-leucine amide following dehydration of the resulting dipeptidyl amide **7** with trifluoro-

* To whom correspondence should be addressed. Tel.: +81-78-997-1010. Fax: +81-78-997-1016. E-mail: shirasaki@senju.co.jp.

† Current address: Faculty of Pharmaceutical Sciences, Kumamoto University, 5-1 Oe-honmachi, Kumamoto 862-0973, Japan.

Scheme 1^a

^a Conditions: (a) L-Leu-NH₂·HCl, EtOAc; (b) (CF₃CO₂)₂O, TEA, THF.

Table 1. Inhibitory Activities against Calpains, Solubility and Metabolic Stability of Aldehyde **1** and Its Analogs **2–5**

Compd	Structure	IC ₅₀ (μM) ^a		Solubility ^b (mg/mL)	Metab. Stab. ^c (%)
		μ-calpain	m-calpain		
2 ^f		0.88 ^d	2.6 ^d	1.5 ^d	79
3 ^f		0.37 ^f	ND ^f	0.21 ^f	64
4 ^f		0.021 ^d	0.021 ^d	0.0053 ^d	25
5		> 100	> 100	ND ^f	ND ^f
1 ^f		0.022 ^d	0.049 ^d	0.10 ^d	3

^a IC₅₀ values are reported as the mean of two independent determinations; errors are within ±20%. ^b Aqueous-solubility in pH 7 buffer, at 25 °C (*n* = 1). ^c Metabolic stability represented in residual percent after incubation with human hepatic S9 fraction for 0.5 h at 37 °C (*n* = 1). ^d Reference 23. ^e Reference 22a. ^f Not determined. ^g Reference 12.

acetic anhydride and Et₃N.²⁴ The synthesis of hemiacetal **8** (SNJ-1715)²³ was also reported previously and hemiacetals **9–18** were prepared by the same method (Table 3, Scheme 2). Boc-protected amino acids (Leu, Val, and Ile) were coupled to homoserine lactone to give intermediates **19–21**. The intermediates were deprotected with 4 M HCl/EtOAc, and the resulting crude amine hydrochloride salts were reacted with various isothiocyanates to give the thiourea intermediates. These were reduced with DIBAL-H, and the resulting compounds were purified by preparative HPLC to provide hemiacetals **9–18** as a mixture of anomers.

Results and Discussion

The aldehyde functionality is an essential active site for hemithioacetal formation by reaction with the SH group on the Cys residue of calpains. The intrinsic instability of aliphatic aldehydes renders them problematic as electrophilic warheads. It is, therefore, desirable to replace the aldehyde with other electrophilic warheads that can reversibly react with the SH group but are more chemically stable than aldehydes. α-Ketoacids, α-ketoesters, α-ketoamides, hydrazones, nitriles, and masked aldehydes such as hydroxyoxazolidines and cyclic hemiacetals have been reported as reversible warheads for calpain inhibitors.^{3,25} α-Ketoacids show very high potency, but generally low membrane permeability.^{25a,26} Most α-ketoesters would be rapidly metabolized to α-ketoacids by esterases in the plasma and tissues.²⁶ We, therefore, selected the cyclic hemiacetal, hydrazone, nitrile, and α-ketoamide for further development (Figure 2).

Table 2. Inhibitory Activities against Calpains, Solubility and Metabolic Stability of Hemiacetal Derivatives

compd	structure			IC ₅₀ (μM) ^a		solubility ^b (mg/mL)	metab. stab. ^c (%)
	P2	R ²	n	μ-calpain	m-calpain		
8 ^d	Leu	H	0	0.086 ^d	0.19 ^d	1.5	100
9	Val	H	0	0.63	1.9	ND ^e	ND ^e
10	Ile	H	0	0.60	1.7	ND ^e	ND ^e
11	Leu	H	1	0.15	0.24	0.60	ND ^e
12	Leu	4-F	0	0.15	0.19	3.3	ND ^e
13	Leu	4-MeO	0	0.22	0.20	2.4	ND ^e
14	Leu	3-CN	0	0.26	0.17	1.5	ND ^e
15	Leu	4-CN	0	0.14	0.12	2.2	ND ^e
16	Leu	2-Me	0	0.24	0.25	1.7	ND ^e
17	Leu	3-Me	0	0.18	0.34	1.3	ND ^e
18	Leu	4-Me	0	0.91	0.17	1.1	ND ^e
2				0.88	1.2	1.5	79

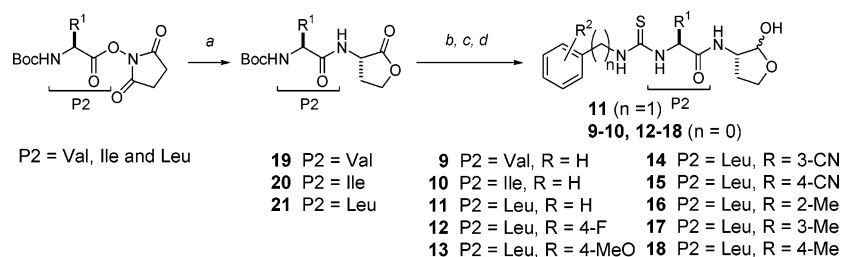
^a IC₅₀ values are reported as the mean of two independent determinations; errors are within ±20%. ^b Aqueous solubility in pH 7 buffer at 25 °C (*n* = 1). ^c Metabolic stability represented in residual percent after the incubation with human hepatic S9 fraction for 0.5 h at 37 °C (*n* = 1). ^d Reference 23. ^e Not determined.

Table 3. In Vitro PK Properties of Hemiacetal **8** and Aldehyde **1**

compd	metab. stab. ^a (%)	Caco-2 ^b <i>P</i> _{app} ^c (10 ⁻⁶ cm·s ⁻¹)	log D ₇ ^d
8	100	14.3	0.70
1	3	2.6	1.7

^a Metabolic stability represented in residual percent after the incubation with human hepatic S9 fraction for 0.5 h at 37 °C (*n* = 1). ^b The Caco-2 cell monolayer permeability assay (*n* = 1) errors of standard compound (propranolol, *n* = 3) are within ±5%. ^c *P*_{app} is the apparent permeability coefficient for the apical to basolateral flux in 10⁻⁶ cm/s. ^d Reference 23.

The corresponding analogues (**2–5**)^{22a,23} of aldehyde lead **1** were evaluated for their metabolic stability against human S9 (Table 2). Cyclic hemiacetal **2**,²³ hydrazone **3**,^{22a} and α-ketoamide **4**²³ demonstrated significantly higher metabolic stability in human S9 than that in **1**. Hemiacetal **2** was the most metabolically stable inhibitor in this series and showed good aqueous solubility. However, the activities were about 50-fold lower than that of **1**. The increase in metabolic stability and the decrease in potency may result from a reduction in both the electrophilicity of the α-carbonyl moiety and the lipophilicity. The decrease in electrophilicity led to a suppression of the nucleophilic attack from both calpains and metabolic enzymes.²⁷ A reduced lipophilicity diminished the affinity of both enzymes by a decrease in hydrophobic interactions.²⁸ Hydrazone **3** also exhibited good metabolic stability presumably due to a decrease in electrophilicity and a high water solubility in acidic conditions. However, it was found to rapidly decompose to aldehyde **1** in simulated gastric juice (pH 1.2). Ketoamide **4** showed improved metabolic stability and very potent inhibitory activity, but it had extremely low aqueous solubility. Nitrile **5** was also

Scheme 2^a

^a Conditions: (a) (*S*)- α -amino- γ -butyrolactone, TEA, DMF; (b) 4 M HCl/EtOAc; (c) R-NCS, TEA, EtOAc; (d) DIBAL-H, CH₂Cl₂.

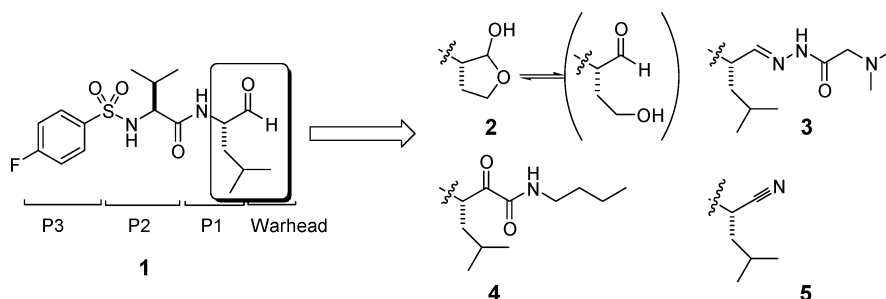


Figure 2. Warhead conversion for the improvement in metabolic stability.

unsuitable because it exhibited a complete loss of calpain inhibitory activity. We focused our efforts accordingly on the modification of the structure of **2** to improve its activity.

We conducted an optimization study of the P2 substituent and P3 *N*-capping group to enhance inhibitory activity. The activities and water solubility of the cyclic hemiacetals are shown in Table 3. The substitution of the 4-*F*-phenylsulfonamide moiety with the phenylthiourea moiety at P3 slightly increased inhibition against μ -calpain (**2** vs **9**). The placement of a Leu residue at P2 was the most effective in inhibiting calpains (**8** vs **9** vs **10**). Leu derivative **8** exhibited a 7-fold higher activity than the Val and Ile derivatives. The P2 substituent SAR was identical to that of *N*-Cbz-dipeptidyl aldehydes⁵ and cyclic hemiacetals previously reported in the literatures.²⁹ The incorporation of a methylene spacer into the phenylthiourea resulted in a 2-fold reduction in potency and aqueous solubility (**8** vs **11**). The various substituents on the phenyl ring of **8** resulted in the decreased inhibitory activity and no significant change in the aqueous solubility (**12**–**18**). Therefore, the nonsubstituted phenyl moiety was optimal. Hemiacetal **8** was the most potent inhibitor in this series, and in addition, its metabolic stability in human S9 was higher than that of parent hemiacetal **2** (Table 2). Furthermore, compound **8** showed good Caco-2 permeability (Table 3).

Pharmacokinetics. Pharmacokinetic properties of hemiacetal **8** and aldehyde lead **1** were determined in rats, and the plasma concentration time profiles after single oral administration are shown in Figure 3. Hemiacetal **8** demonstrated a rapid absorption ($T_{\max} = 0.25$ h) and an increased AUC (based on dose normalized values) compared to those of **1**. The pharmacokinetic parameters of **8** and **1** after single oral and intravenous (iv) administrations are summarized in Table 4. Hemiacetal **8** showed excellent oral bioavailability ($F = 66\%$) and an improved iv terminal half-life ($t_{1/2} = 1.9$ h). The plasma clearance (55 mL/min/kg) and volume of distribution (2.3 L/kg) of **8** were lower than those of **1** (89 mL/min/kg, 6.1 L/kg). We considered that the improvement of *in vitro* hepatic stability was associated with the decline in plasma total clearance and first pass metabolism. Furthermore, hemiacetal **8** showed adequate aqueous solubility and high Caco-2 permeability for oral absorption (Table 3). The permeability of **8** was higher

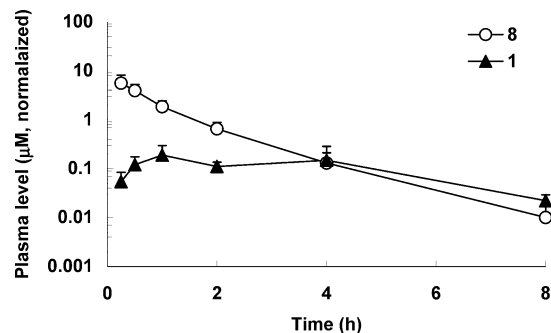


Figure 3. Plasma levels of **1** (po 500 mg/kg) and **8** (po 10 mg/kg) via single oral administration in rats. Each value represents the mean \pm SD ($n = 4$ –5, dose normalized to 10 mg/kg).

Table 4. PK Parameters of Hemiacetal **8** and Aldehyde **1** in Rats

parameters ^a	8		1	
	iv/3	po/10	iv/3	po/500
number of animals	5	5	4	4
(<i>n</i> /time point)				
AUC ^b ($\mu\text{M}\cdot\text{h}$)	2.6 \pm 0.1	5.7 \pm 0.4	1.5 \pm 0.3	45 \pm 11
C_{\max} (μM)		5.6 \pm 2.5		9.4 \pm 5.4
T_{\max} (h) (median)		0.25		1.0
$t_{1/2}$ ^c (h)	1.9 \pm 0.7		0.7 \pm 0.8	
V_{ss} ^d (L/kg)	2.3 \pm 0.3		6.1 \pm 4.0	
CL ^e (mL/min/kg)	55 \pm 2.7		89 \pm 86	
F ^f (%)		66 \pm 7.3		18 \pm 4.5

^a The values are mean \pm SD. ^b The area under the curves for 0 h to infinity. ^c The terminal half-life. ^d The steady-state volume of distribution. ^e The total clearance. ^f Oral bioavailability.

than that of **1**, even though **8** had lower lipophilicity (**8**, log $D_7 = 0.70$; **1**, log $D_7 = 1.7$).²³ The reason for this may be attributed to a reduced reactivity. The aldehyde group may react with various membrane substances that contain nucleophiles such as an NH or SH group.²⁷ A decrease in the reactivity on replacement of the aldehyde with the hemiacetal resulted in an increase in membrane permeability. Therefore, the enhancement of the oral BA of **8** is ascribed to an improvement in these parameters. The prolongation of the terminal half-life of **8** was caused by a reduced plasma clearance, which predominated over a reduction in the volume of distribution. Thus, the replacement of the aldehyde moiety with the cyclic hemiacetal significantly

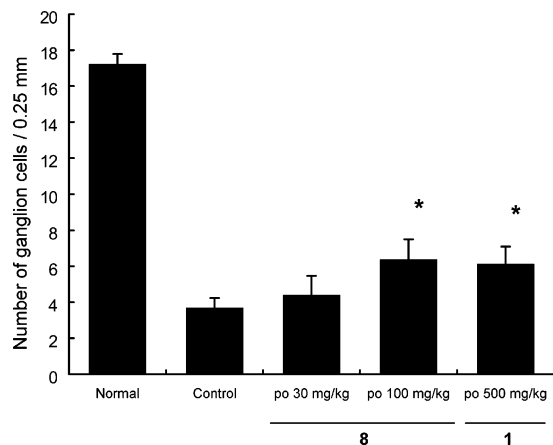


Figure 4. Cell density in the retinal ganglion cell layer seven days after retinal ischemia. Each column represents the mean \pm SEM for eight rats. *: $p < 0.05$, significantly different from the control group (student's t -test).

improved the BA and the terminal half-life through the enhancement of metabolic stability, aqueous solubility, and membrane permeability.

Retinal Ischemia Model in Rats. We evaluated the neuroprotective efficacy of hemiacetal **8** and aldehyde lead **1** in the ischemia–reperfusion model in rats.¹⁹ As shown in Figure 4, **8** demonstrated a significant effect at po 100 mg/kg (the cell density in the retinal ganglion cell layer: **8** vs control; 6.38 ± 3.36 vs 3.69 ± 1.65 , $p < 0.05$) and no effect at po 30 mg/kg (4.41 ± 3.18 vs 3.69 ± 1.65 , not statistically significant, student t -test). Compound **8** is effective only at a 5-fold lower dose compared to that of **1** (po 500 mg/kg). Hemiacetal **8** showed a 3-fold higher oral BA ($F = 66\%$) than that of lead **1** ($F = 18\%$), although **8** displayed 4-fold less in vitro potency. Improvement of oral BA led to an enhanced retinal efficacy.

Conclusion

On the basis of the assumption that the presence of the aldehyde moiety on potent lead **1** decreased oral bioavailability through its metabolic lability, we replaced the aldehyde moiety with a more chemically stable warhead. The resulting inhibitors, cyclic hemiacetal **2**, hydrazone **3**, and α -ketoamide **4**, showed higher in vitro metabolic stability compared to that of **1**. Hemiacetal **2** was the most metabolically stable compound with only a modest loss of potency. Optimization of **2** at the P2/P3 sites led to hemiacetal **8** with an improved inhibitory activity. In addition, **8** had excellent metabolic stability, oral BA ($F = 66\%$), and a prolonged half-life. Furthermore, **8** was efficacious in the rat retinal ischemia model at a 5-fold lower oral dose than that of **1**. Hemiacetal **8** is a useful tool for exploration of orally active drugs for the treatment of retinal diseases. In future work, it will be evaluated by the appropriate pharmacological models that reflect clinical efficacy.

Experimental Section

General. All reagents were of commercial grade and used without further purification. Melting points were obtained using a Yanaco micro melting point apparatus without correction. ¹H NMR and ¹³C NMR spectra were measured using a Varian Gemini-2000 Spectrometer. Chemical shifts were reported in parts per million (δ value), and coupling constants (J) were reported in hertz. Tetramethylsilane (δ 0) and DMSO (δ 39.7) were used as internal standards (¹H NMR and ¹³C NMR, respectively). Splitting patterns are indicated as follows: s, singlet; d, doublet; t, triplet; q, quartet; m, multiplet; br, broad peak. The NMR spectra of cyclic hemiacetals were extremely complicated because of the presence of anomeric

carbon. The major and minor peaks of the same proton were separately listed, in case each peak was identified. Specific rotations were measured with a Horiba SEPA-2000 model. Matrix-assisted laser desorption ionization time-of-flight mass spectrometry (MALDI-TOF MS) were obtained on a Perceptive Voyager DE PRO using α -cyano-4-hydroxycinnamic acid as a matrix. Analytical HPLC was performed with a Shimadzu Class LC-10A system (LC-10AD, SPD-10A, SIL-10A, CTO-10A, CBM-10A). Preparative HPLC was performed using two Shimadzu LC-8A pumps with an SPD-6AV UV–Vis detector set at 250 nm. Elemental analyses were performed on an Elementar Vario EL analyzer.

***N*-(4-Fluorophenylsulfonyl)-L-valyl-L-leucinamide (7).** *N*-(4-Fluorophenylsulfonyl)-L-valine *N*-hydroxysuccinimide ester (6.0 g, 16 mmol) (**6**) was dissolved in EtOAc (200 mL), and L-leucinamide HCl (3.2 g, 19 mmol) and Et₃N (3.3 g, 32 mmol) were added thereto. The mixture was stirred at room temperature for 18 h. After the reaction occurred, 1 M HCl was added, and the precipitate was dissolved in EtOAc. The organic layer was washed with 1 M HCl, saturated NaHCO₃, and saturated NaCl, dried over MgSO₄, and concentrated in vacuo. The solid was washed with hexane/EtOAc (1:1) to give **7** (5.2 g, 83%) as colorless crystals. Mp 224.0–225.0 °C. ¹H NMR (300 MHz, DMSO-*d*₆) δ 0.70 (d, 3H, $J = 5.7$ Hz), 0.76 (d, 3H, $J = 6.9$ Hz), 0.79 (d, 3H, $J = 5.7$ Hz), 0.80 (d, 3H, $J = 6.9$ Hz), 1.16–1.27 (m, 3H), 1.82 (m, 1H), 3.55 (m, 1H), 3.94–4.02 (m, 1H), 6.89 (s, 1H), 7.24 (s, 1H), 7.30–7.36 (m, 2H), 7.77–7.83 (m, 3H), 7.87 (d, 1H, $J = 8.4$ Hz).

***N*-(1-Cyano-3-methylbutyl)-2-((4-fluorophenyl)sulfonyl)-3-methylbutanamide (5).** Compound **7** (2.0 g, 5.2 mmol) was dissolved in THF (50 mL), and Et₃N (1.0 g, 10 mmol) and trifluoroacetic anhydride (1.2 g, 5.7 mmol) were added under ice-cold conditions. The mixture was stirred under the same conditions for 2 h. After the reaction occurred, the mixture was evaporated, and the residue was dissolved in EtOAc. The solution was washed with 1 M HCl, saturated NaHCO₃, and saturated NaCl, dried over MgSO₄, and concentrated in vacuo. The residue recrystallized from EtOAc to give **5** (0.82 g, 43%) as colorless crystals. ¹H NMR (300 MHz, DMSO-*d*₆) δ 0.77 (d, 3H, $J = 6.3$ Hz), 0.79–0.83 (m, 9H), 1.25–1.54 (m, 3H), 1.81 (m, 1H), 3.43 (dd, 1H, $J = 9.3, 7.9$ Hz), 4.34 (dt, 1H, $J = 15.5, 7.5$ Hz), 7.30–7.40 (m, 2H), 7.76–7.81 (m, 2H), 8.14 (d, 1H, $J = 9.3$ Hz), 8.67 (d, 1H, $J = 7.5$ Hz). Anal. (C₁₇H₂₄FN₃O₃S) C, H, N.

General Procedure for the Synthesis of Butyrolactone Compounds 19–20. (2*S*)-2-((*tert*-Butoxy)carbonylamino)-3-methyl-*N*-((3*S*)-tetrahydro-2-oxo-3-furanyl)butanamide (**19**). To a solution of *N*-Boc-valine *N*-hydroxysuccinimide ester (17 g, 54 mmol) in DMF (60 mL) was added (*S*)-(-)- α -aminobutyrolactone hydrobromide (L-homoserine lactone hydrobromide) (15 g, 81 mmol) and Et₃N (16 g, 162 mmol) under ice-cold conditions. The mixture was stirred at room temperature for 18 h. The mixture was diluted with EtOAc, and the solution was washed with 1 M HCl, saturated NaHCO₃, and saturated NaCl, dried over MgSO₄, and concentrated in vacuo. The residue was crystallized from hexane to give **19** (13 g, 82%) as colorless crystals. Mp 113.9–114.9 °C. ¹H NMR (300 MHz, DMSO-*d*₆) δ 0.84 (d, 3H, $J = 6.9$ Hz), 0.87 (d, 3H, $J = 6.9$ Hz), 1.38 (s, 9H), 1.93 (m, 1H), 2.17 (m, 1H), 2.39 (m, 1H), 3.78 (dd, 1H, $J = 8.9$ Hz, 7.2 Hz), 4.21 (m, 1H), 4.40 (m, 1H), 4.60 (m, 1H), 6.68 (d, 1H, $J = 8.9$), 8.37 (d, 1H, $J = 7.8$ Hz).

(2*S*)-2-((*tert*-Butoxy)carbonylamino)-3-methyl-*N*-((3*S*)-tetrahydro-2-oxo-3-furanyl)pentanamide (**20**). Colorless crystals. Mp 156.4–159.2 °C. ¹H NMR (300 MHz, CDCl₃) δ 0.90 (3H, t, $J = 7.5$ Hz), 0.95 (d, 3H, $J = 6.6$ Hz), 1.15 (m, 1H), 1.43 (s, 9H), 1.50 (m, 1H), 1.88 (m, 1H), 2.21 (m, 1H), 2.73 (m, 1H), 4.01 (m, 1H), 4.26 (m, 1H), 4.46 (td, 1H, $J = 9.0$ Hz, 1.2 Hz), 4.54 (m, 1H), 5.11 (d, 1H, $J = 8.7$ Hz), 6.87 (m, 1H).

General Procedure for the Synthesis of Cyclic Hemiacetals 9–18. (2*S*)-3-Methyl-2-(((phenylamino)thioxomethyl)amino)-*N*-((3*S*)-tetrahydro-2-hydroxy-3-furanyl)butanamide (**9**). To a solution of **19** (3.0 g, 10 mmol) in EtOAc (100 mL) was added 4 M HCl in EtOAc (10 mL) under ice-cold conditions. The mixture was stirred at room temperature for 18 h (oil-down was observed). The solvent was removed in vacuo, and then EtOAc was added and

removed in vacuo (twice). The resulting oil was suspended with EtOAc, and phenyl isothiocyanate (1.35 g, 10 mmol) and Et₃N (4.8 g, 48 mmol) were added. The mixture was stirred at room temperature for 3 h and washed with 1 M HCl, saturated NaHCO₃ and saturated NaCl, dried over MgSO₄, and evaporated in vacuo to give the thiourea intermediate (2.9 g, 86%, 8.6 mmol) as a white solid, which was used directly in the subsequent reaction without further purification.

To a solution of the resulting thiourea in CH₂Cl₂ (150 mL) was added DIBAL-H (1.0 M solution in toluene) (26 mL, 26 mmol) at -78 °C. The mixture was stirred below -70 °C for 3 h, and saturated NH₄Cl solution (3.0 mL) was added and stirred for 30 min. MgSO₄ and EtOAc (150 mL) were added, and the inorganic was filtered off (using Celite). After concentration in vacuo, the residue was purified with HPLC system (column; YMC-Pack ODS-A 250 × 20 mm, eluent CH₃CN/H₂O/TFA = 30:70:0.1). The main fractions were collected and extracted with EtOAc. The extract was washed with saturated NaHCO₃ and saturated NaCl, dried over MgSO₄, and concentrated in vacuo. The resulting residue was crystallized from hexane to give **9** (1.3 g, 44%) as colorless crystals. Mp 50.9–51.9 °C. [α]_D²⁵ +39.8° (c = 0.2, DMSO). ¹H NMR (300 MHz, DMSO-*d*₆) δ 0.86–0.92 (m, 6H), 1.80 (m, 1H), 2.03–2.26 (m, 2H), 3.69/3.89 (m/m, 1H), 3.93–3.97 (m, 2H), 4.92 (m, 1H), 5.02/5.13 (d/t, 1H, *J* = 4.5/4.7 Hz), 6.16/6.31 (d/d, 1H, *J* = 4.5/4.8 Hz), 7.10 (m, 1H), 7.29–7.34 (m, 2H), 7.52–7.55 (m, 2H), 7.71 (m, 1H), 8.24/7.92 (d/d, 1H, *J* = 6.6/7.5 Hz), 9.82 (s, 1H), major/minor = 1.0:0.83. ¹³C NMR (75 MHz, DMSO-*d*₆) δ 18.3/18.5, 18.9/19.0, 27.8/28.9, 31.4/31.6, 52.1/56.0, 61.2/61.3, 64.0/65.3, 94.0/100.8, 122.9 (2C), 124.2, 128.7 (2C), 139.6, 170.6, 180.5/180.6. MALDI-TOF MS calcd for C₁₆H₂₃N₃O₃S [M + Na]⁺, 360.136; found, 360.137.

(2S,3S)-3-Methyl-2-(((phenylamino)thioxomethyl)amino)-N-((3S)-tetrahydro-2-hydroxy-3-furanyl)pentanamide (10). Colorless crystals. Mp 51.3–52.9 °C. [α]_D²⁵ +33.6° (c = 0.2, DMSO). ¹H NMR (300 MHz, DMSO-*d*₆) δ 0.81–0.87 (m, 6H), 1.03 (m, 1H), 1.48 (m, 1H), 1.68–1.86 (m, 2H), 2.11 (m, 1H), 3.48/3.86 (m/m, 1H), 3.91–3.96 (m, 2H), 4.88 (m, 1H), 4.99/5.10 (d/t, 1H, *J* = 4.5/4.5 Hz), 6.13/6.27 (d/d, 1H, *J* = 4.5/4.2 Hz), 7.07 (m, 1H), 7.27–7.32 (m, 2H), 7.49–7.52 (m, 2H), 7.70/7.71 (d/d, 1H, *J* = 8.4/8.1 Hz), 7.85/8.21 (d/d, 1H, *J* = 7.8/6.6 Hz), 9.76 (s, 1H), major/minor = 1.0:0.77. ¹³C NMR (75 MHz, DMSO-*d*₆) δ 11.69, 15.3/15.4, 24.7/24.9, 27.8/28.9, 37.9/38.1, 52.1/56.0, 60.8/61.0, 64.0/65.3, 94.0/100.8, 122.8 (2C), 124.2, 128.6 (2C), 139.6, 170.6, 180.4/180.4. MALDI-TOF MS calcd for C₁₇H₂₅N₃O₃S [M + Na]⁺, 374.151; found, 374.185.

(2S)-2-((Benzylamino)thioxomethyl)amino)-4-methyl-N-((3S)-tetrahydro-2-hydroxy-3-furanyl)pentanamide (11). Colorless crystals. Mp 62.2–64.4 °C. [α]_D²⁵ +18.9° (c = 0.2, DMSO). ¹H NMR (300 MHz, DMSO-*d*₆) δ 0.84–0.89 (m, 6H), 1.44–1.82 (m, 4H), 2.14 (m, 1H), 3.68/4.03 (m/m, 1H), 3.85–3.97 (m, 2H), 4.66 (bs, 1H), 4.85 (m, 1H), 4.99/5.11 (d/t, 1H, *J* = 4.5/4.4 Hz), 6.12/6.34 (d/bs, 1H, *J* = 4.8 Hz), 7.22–7.36 (m, 5H), 7.58 (m, 1H), 7.68/8.13 (brs, 1H), 7.96 (brs, 1H), major/minor = 1.0:0.80. ¹³C NMR (75 MHz, DMSO-*d*₆) δ 22.4/22.5, 23.1/23.2, 24.4/24.5, 28.1/29.2, 42.1, 47.2, 51.9/56.0, 55.8, 64.1/65.2, 94.0/100.8, 127.1/127.4, 127.4 (2C), 128.5 (2C), 139.3, 172.1, 182.8. MALDI-TOF MS calcd for C₁₈H₂₇N₃O₃S [M + Na]⁺, 388.167; found, 388.162.

(2S)-2-(((4-Fluorophenyl)amino)thioxomethyl)amino)-4-methyl-N-((3S)-tetrahydro-2-hydroxy-3-furanyl)pentanamide (12). Colorless crystals. Mp 77.2–78.3 °C. [α]_D²⁵ +20.1° (c = 0.2, DMSO). ¹H NMR (300 MHz, DMSO-*d*₆) δ 0.90 (d, 6H, *J* = 6.3 Hz), 1.48–1.91 (m, 4H), 2.14 (m, 1H), 3.69/3.95 (m/m, 1H), 3.86–3.91 (m, 2H), 4.93 (m, 1H), 5.00/5.12 (d/t, 1H, *J* = 5.1/4.5 Hz), 6.15/6.34 (d/d, 1H, *J* = 4.8/3.9 Hz), 7.12–7.18 (m, 2H), 7.46–7.52 (m, 2H), 7.73/7.77 (d/d, 1H, *J* = 8.1/7.8 Hz), 7.84/8.25 (d/d, 1H, *J* = 7.8/7.2 Hz), 9.64 (s, 1H), major/minor = 1.0:0.85. ¹³C NMR (75 MHz, DMSO-*d*₆) δ 22.5/22.6, 23.1/23.2, 24.4/24.5, 28.1/29.1, 41.7/42.0, 52.0/56.0, 55.7, 64.1/65.3, 94.0/100.8, 115.1/115.4 (2C), 125.3 (2C), 135.9/136.0, 157.4/160.6, 171.9, 180.6. MALDI-TOF MS calcd for C₁₇H₂₄FN₃O₃S [M + Na]⁺, 392.142; found, 392.141.

(2S)-2-(((4-Methoxyphenyl)amino)thioxomethyl)amino)-4-methyl-N-((3S)-tetrahydro-2-hydroxy-3-furanyl)pentanamide (13). Colorless crystals. Mp 67.9–68.8 °C. [α]_D²⁵ +19.9° (c = 0.2, DMSO). ¹H NMR (300 MHz, DMSO-*d*₆) δ 0.88–0.91 (m, 6H), 1.47–1.87 (m, 4H), 2.14 (m, 1H), 3.69/3.94 (m/m, 1H), 3.74 (s, 3H), 3.86–3.90 (m, 2H), 4.89 (m, 1H), 4.99/5.11 (d/t, 1H, *J* = 4.8/4.4 Hz), 6.15/6.35 (d/d, 1H, *J* = 4.8/4.2 Hz), 6.88–6.91 (m, 2H), 7.28–7.33 (m, 2H), 7.47/7.53 (d/d, 1H, *J* = 8.1/6.9 Hz), 8.22/7.81 (d/d, 1H, *J* = 6.6/7.8 Hz), 9.49 (s, 1H), major/minor = 1.0:0.78. ¹³C NMR (75 MHz, DMSO-*d*₆) δ 22.5/22.7, 23.1/23.2, 24.4/24.5, 28.0/29.1, 41.7/42.0, 52.0/56.0, 55.4/55.9, 55.7, 64.1/65.3, 94.0/100.8, 114.0 (2C), 125.5 (2C), 132.1, 172.0, 180.5/180.7. MALDI-TOF MS calcd for C₁₈H₂₇N₃O₃S [M + Na]⁺, 404.162; found, 404.166.

(2S)-2-(((3-Cyanophenyl)amino)thioxomethyl)amino)-4-methyl-N-((3S)-tetrahydro-2-hydroxy-3-furanyl)pentanamide (14). Colorless crystals. Mp 54.1–55.1 °C. [α]_D²⁵ +23.8° (c = 0.2, DMSO). ¹H NMR (300 MHz, DMSO-*d*₆) δ 0.90–0.92 (m, 6H), 1.45–1.90 (m, 4H), 2.15 (m, 1H), 3.69/3.96 (m/m, 1H), 3.86–3.91 (m, 2H), 4.93 (m, 1H), 5.01/5.12 (d/t, 1H, *J* = 4.8/4.5 Hz), 6.16/6.34 (d/d, 1H, *J* = 4.8/4.5 Hz), 7.48–7.54 (m, 2H), 7.75 (m, 1H), 8.06–8.18 (m, 2H), 8.30/7.92 (d/d, 1H, *J* = 6.9/7.5 Hz), 9.93 (s, 1H), major/minor = 1.0:0.75. ¹³C NMR (75 MHz, DMSO-*d*₆) δ 22.5/22.6, 23.1/23.2, 24.5/24.5, 27.9/29.2, 41.6/41.9, 52.1/56.0, 55.7, 64.1/65.3, 94.0/100.8, 111.2, 118.9, 125.1, 127.1, 130.0 (2C), 140.8, 171.7, 180.2/180.4. MALDI-TOF MS calcd for C₁₈H₂₄N₃O₃S [M + Na]⁺, 399.147; found, 399.167.

(2S)-2-(((4-Cyanophenyl)amino)thioxomethyl)amino)-4-methyl-N-((3S)-tetrahydro-2-hydroxy-3-furanyl)pentanamide (15). Colorless crystals. Mp 80.0–82.9 °C. [α]_D²⁵ +51.2° (c = 0.2, DMSO). ¹H NMR (300 MHz, DMSO-*d*₆) δ 0.89–0.92 (m, 6H), 1.50–1.90 (m, 4H), 2.14 (m, 1H), 3.69/3.96 (m/m, 1H), 3.86–3.91 (m, 2H), 4.93 (m, 1H), 5.01/5.12 (d/t, 1H, *J* = 5.1/4.5 Hz), 6.16/6.33 (d/d, 1H, *J* = 4.5/4.2 Hz), 7.73–7.76 (m, 2H), 7.84–7.88 (m, 2H), 8.18 (m, 1H), 8.31/7.95 (d/d, 1H, *J* = 6.6/7.8 Hz), 10.10 (s, 1H), major/minor = 1.0:0.75. ¹³C NMR (75 MHz, DMSO-*d*₆) δ 22.4/22.5, 23.0/23.1, 24.4/24.5, 27.9/29.2, 41.5/41.7, 52.0/56.1, 55.6, 64.0/65.2, 94.0/100.8, 104.9, 119.2, 121.2 (2C), 132.8 (2C), 144.4, 171.5, 179.7. MALDI-TOF MS calcd for C₁₈H₂₄N₃O₃S [M + Na]⁺, 399.147; found, 399.150.

(2S)-4-Methyl-2-(((2-methylphenyl)amino)thioxomethyl)amino)-N-((3S)-tetrahydro-2-hydroxy-3-furanyl)pentanamide (16). Colorless crystals. Mp 57.9–58.9 °C. [α]_D²⁵ +9.8° (c = 0.2, DMSO). ¹H NMR (300 MHz, DMSO-*d*₆) δ 0.88–0.91 (m, 6H), 1.48–1.86 (m, 4H), 2.16 (m, 1H), 2.17 (s, 3H), 3.69/3.94 (m/m, 1H), 3.86–3.90 (m, 2H), 4.91 (m, 1H), 4.98/5.11 (d/t, 1H, *J* = 4.5/4.5 Hz), 6.15/6.36 (d/d, 1H, *J* = 4.8/3.9 Hz), 7.12–7.31 (m, 4H), 7.46/7.52 (d/d, 1H, *J* = 8.4/9.9 Hz), 7.78/8.19 (d/d, 1H, *J* = 7.2/6.6 Hz), 9.20 (s, 1H), major/minor = 1.0:0.89. ¹³C NMR (75 MHz, DMSO-*d*₆) δ 17.8, 22.5/22.7, 23.1/23.2, 24.5/24.5, 28.1/29.1, 41.5/41.9, 51.9/56.0, 56.0, 64.1/65.2, 94.0/100.8, 126.3, 126.5, 127.9, 130.6, 134.5, 137.4, 171.9, 181.2/181.3. MALDI-TOF MS calcd for C₁₈H₂₇N₃O₃S [M + Na]⁺, 388.167; found, 388.176.

(2S)-4-Methyl-2-(((3-methylphenyl)amino)thioxomethyl)amino)-N-((3S)-tetrahydro-2-hydroxy-3-furanyl)pentanamide (17). Colorless crystals. Mp 61.4–61.9 °C. [α]_D²⁵ +4.8° (c = 0.2, DMSO). ¹H NMR (300 MHz, DMSO-*d*₆) δ 0.91 (d, 6H, *J* = 6.3 Hz), 1.47–1.88 (m, 4H), 2.12 (m, 1H), 2.28 (s, 3H), 3.69/3.95 (m/m, 1H), 3.86–3.91 (m, 2H), 4.92 (m, 1H), 5.00/5.11 (d/t, 1H, *J* = 4.8/4.5 Hz), 6.15/6.34 (d/d, 1H, *J* = 4.8/4.5 Hz), 6.92 (m, 1H), 7.17–7.30 (m, 3H), 7.68/7.74 (d/d, 1H, *J* = 8.4/7.8 Hz), 8.24/7.84 (d/d, 1H, *J* = 6.6/7.5 Hz), 9.63 (s, 1H), major/minor = 1.0:0.87. ¹³C NMR (75 MHz, DMSO-*d*₆) δ 21.2, 22.5/22.6, 23.1/23.2, 24.5/24.5, 28.0/29.1, 41.6/42.0, 52.0/56.0, 55.6/55.8, 64.1/65.3, 94.0/100.8, 120.1, 123.4, 125.0, 128.5, 138.0, 139.4, 171.9, 180.1/180.3. MALDI-TOF MS calcd for C₁₈H₂₇N₃O₃S [M + Na]⁺, 388.167; found, 388.175.

(2S)-4-Methyl-2-(((4-methylphenyl)amino)thioxomethyl)amino)-N-((3S)-tetrahydro-2-hydroxy-3-furanyl)pentanamide (18). Colorless crystals. Mp 87.3–88.7 °C. [α]_D²⁵ +23.9° (c = 0.2, DMSO). ¹H NMR (300 MHz, DMSO-*d*₆) δ 0.89 (d, 6H, *J* = 6.6

Hz), 1.36–1.85 (m, 4H), 2.14 (m, 1H), 2.21 (s, 3H), 3.68/3.94 (m, 1H), 3.85–3.90 (m, 2H), 4.28 (m, 1H), 4.98/5.10 (d/t, 1H, $J = 4.8/4.7$ Hz), 6.14/6.33 (d/d, 1H, $J = 4.5/3.6$ Hz), 6.24 (m, 1H), 7.01–7.03 (m, 2H), 7.23–7.26 (m, 2H), 8.19/7.84 (d/d, 1H, $J = 7.2/7.8$ Hz), 8.46 (s, 1H), major/minor = 1.0:0.46. ^{13}C NMR (75 MHz, DMSO- d_6) δ 20.4, 22.1/22.3, 23.2/23.4, 24.4/24.5, 27.9/29.1, 42.5/42.8, 51.1/51.2, 51.9/55.9, 64.1/65.3, 94.0/100.9, 117.7 (2C), 129.3 (2C), 130.0, 138.0, 154.9, 172.8. MALDI-TOF MS calcd for $\text{C}_{18}\text{H}_{27}\text{N}_3\text{O}_3\text{S} [\text{M} + \text{Na}]^+$, 388.167; found, 388.165.

Inhibition Assays for Calpains. The inhibition assays were performed as described in the literature^{22,30} using commercial μ -calpain (human erythrocyte, Calbiochem) and m-calpain (porcine kidney, Calbiochem). An assay solution containing 0.5 mg/mL of casein, 20 mM dithiothreitol, 50 mM Tris-HCl (pH 7.4), and 1.0 nmol of enzyme was used. The assay solution (200 μL) and DMSO (2.5 μL) containing inhibitors of different concentrations were placed in each well. The reaction was started by the addition of 20 mM CaCl_2 (50 μL) in a test well and 1 mM EDTA (50 μL) in a blank well. After incubation for 60 min at 30 °C, the mixture (100 μL) was transferred to another plate, and H_2O (100 μL) and Bio-Rad protein assay dye reagent (50 μL) were placed in each well. After incubation at room temperature for 15 min, the OD of the mixture at 595 nm was recorded on a plate reader (Multiscan Multisoft, Labsystems). The percent inhibition was calculated from the differences in the ODs between when the compound was present and when it was absent.

Metabolic Stability. Human hepatic S9 incubations were performed in the presence of an NADPH-generating system composed of 3 mM MgCl_2 , 1 mM NADP^+ , 5 mM glucose-6-phosphate, and 1 Unit/mL of glucose-6-phosphate dehydrogenase in a 50 mM potassium phosphate buffer (pH 7.4). The human S9 prepared by XenoTech LLC (Lenexa, KS) was purchased from the Nosan Corporation (Yokohama, Japan). All concentrations are relative to the final incubation volume (5 mL). The compounds were added in acetonitrile to a final concentration of 5 μM . The incubations were conducted at 37 °C. After 30 min, 1 mL of the incubations were sampled, and the reaction was terminated by the addition of 4 mL of acetonitrile. The precipitated proteins were removed by centrifugation, the supernatants were evaporated, and the residue was dissolved in mobile phase. The solution was analyzed by LC-UV or LC-MS/MS.

Pharmacokinetic Studies in Rats. The in vivo pharmacokinetic results were determined after oral or intravenous (po 10 or 500 mg/kg or iv 3 mg/kg) single agent dosing to male Sprague–Dawley rats ($n = 4$ or 5/time point, weight 200–250 g). Each compound (**1** or **8**) was formulated as a suspension in 0.5% carboxymethyl cellulose solution (CMC) for oral administration. In the case of iv administration, each compound was dissolved in a vehicle consisting of 60% poly(ethylene glycol) and 40% water at a concentration of 10 mg/mL. The animals were anesthetized with isoflurane at predetermined times (0.1 (iv only), 0.25, 0.5, 1, 2, 4, and 8 h), and the blood was sampled from the abdominal aorta into heparinized syringes. The blood was centrifuged to obtain plasma. All plasma samples were frozen and stored at –30 °C until analysis. The frozen solution was fused at room temperature, and test sample solutions were prepared by a solid-phase extraction procedure using OASIS HLB (60 mg) cartridges by Waters. The plasma concentration of each test compound was determined by turboionspray on an Applied Biosystems/MDS-Sciex API 4000 triple-quadrupole mass spectrometer equipped with a turbo ion spray source using multiple reaction monitoring (MRM). The samples were chromatographed on a NANOSPACE SI-2 (Shiseido) HPLC system with Shiseido Capcell pak C18 MG-II column (75 \times 1.5 mm, 5 μm) at 40 °C using a mobile phase ($\text{MeOH}/\text{H}_2\text{O}/\text{HCO}_2\text{H} = 40:60:0.1$, for compound **1**) or Shiseido Capcell pak C18 ACR (150 \times 1.5 mm, 3 μm) at 40 °C using a mobile phase ($\text{MeCN}/\text{H}_2\text{O} = 70:30$, for compound **8**) at a flow rate of 0.20 mL/min. Data reduction was performed using MDS-Sciex Analyst ver. 1.3 software. The noncompartmental model was used to calculate pharmacokinetic parameters from the resulting plasma concentration vs time profiles using WinNonLin (Scientific Consulting, Inc.).

Solubility Determination. A suspension of test compound in 2.0 mL of buffer solution (pH 7.0) or simulated gastric juice (pH 1.2) was shaken at 25 °C for 5 h. The suspension was filtered through CHROMATODISK (0.45 μm , GL Sciences), and the filtrate (1.0 mL) was made exactly 10 mL by the addition of the mobile phase as a sample solution. The measurement was performed with 20 μL each of the sample solution and the standard solution under analytical HPLC according to the following conditions: wavelength, UV 250 nm; column, YMC-Pack ODS A-303 (250 \times 4.6 mm, 5 μm); column temperature, 45 °C; mobile phase, $\text{CH}_3\text{CN}/\text{H}_2\text{O}/\text{TFA} = 40:60:0.1$; and flow rate, 1.0 mL/min. The concentration of the test compound in the sample solution was calculated from the ratio of the peak area in the sample solution and the standard solution.

Retinal Ischemia–Reperfusion Model in Rats.¹⁹ Male Sprague–Dawley rats (150–250 g) were used, and the compounds formulated as a suspension in 0.5% CMC solution were orally administered to rats 15 min before ischemia (**1**, 500 mg/kg; **8**, 30 and 100 mg/kg). The control group received the vehicle solution. The rats were anesthetized with an intraperitoneal injection of sodium pentobarbital (60 mg/kg). The body temperature was maintained at 37 °C. Retinal ischemia on the left eye was produced by the occlusion of the central retina and posterior ciliary arteries with a clip. After retinal ischemia was produced for 55 min, the clip was removed. The retinal arteries were allowed to reperfuse. A sham operation was performed on the right eye without ligation. After reperfusion, the same dose of compounds was orally administered. The efficacy was evaluated by a measurement of cell density in the retinal ganglion cell layer 1–2 mm from the optic disk. The cells were stained with hematoxylin and eosin (HE staining). The number of cell nuclei in the ganglion cell layers was counted at a width of 250 μm at three sites.

Acknowledgment. We thank Dr. Wataru Takayama, Yusuke Sakai, and Noriko Nada for supporting our laboratory work. In addition, we thank Dr. Yukuo Yoshida and Akiko Shirasaki for the critical reading of this manuscript. Also, we thank Drs. Yutaka Kawamatsu and Mitsuyoshi Azuma for useful discussions.

Supporting Information Available: Elemental analyses for compound **5**. HPLC analysis data for compounds **9–18**. This material is available free of charge via the Internet at <http://pubs.acs.org>.

References

- (1) (a) Ono, Y.; Sorimachi, H.; Suzuki, K. Pharmacology and toxicology of calcium-dependent protease. In *Calpain*; Wang, K. K. W., Yuen, P.-W., Eds.; Taylor & Francis: Philadelphia, 1999; pp1–3. (b) Huang, Y.; Wang, K. K. The calpain family and human disease. *Trends Mol. Med.* **2001**, *7*, 355–362.
- (2) (a) Wang, K. K. W.; Yuen, P.-W. Calpain inhibition: an overview of its therapeutic potential. *Trends Pharmacol. Sci.* **1994**, *15*, 412–419. (b) Stracher, A. Calpain inhibitors as therapeutic agents in nerve and muscle degeneration. *Ann. N.Y. Acad. Sci.* **1999**, *884*, 52–59. (c) Yuen, P.-W.; Wang, K. K. W. Therapeutic potential of calpain inhibitors in neurodegenerative disorders. *Expert Opin. Invest. Drugs* **1996**, *5*, 1291–1304. (d) Zatz, M.; Starling, A. Calpains and disease. *N. Engl. J. Med.* **2005**, *352*, 2413–2423.
- (3) (a) Donkor, I. O. A survey of calpain inhibitors. *Curr. Med. Chem.* **2000**, *7*, 1171–1188. (b) Wells G. J.; Bihovsky, R. Calpain inhibitors as potential treatment for stroke and other neurodegenerative disease: recent trends and developments. *Expert Opin. Ther. Pat.* **1998**, *8*, 1707–1727 (c) Leung, D.; Abbenante, G.; Fairlie, D. P. Protease inhibitors: current status and future prospects. *J. Med. Chem.* **2000**, *43*, 305–341.
- (4) (a) Sasaki, T.; Kikuchi, T.; Yumoto, N.; Yoshimura, N.; Murachi, T. Comparative specificity and kinetic studies on porcine calpain I and calpain II with naturally occurring peptides and synthetic fluorogenic substrates. *J. Biol. Chem.* **1984**, *259*, 12489–12494. (b) Tompa, P.; Buzder-Lantos, P.; Tantos, A.; Farkas, A.; Szilágyi, A.; Bánóczy, Z.; Hudecz, F.; Friedrich, P.; On the sequential determinants of calpain cleavage. *J. Biol. Chem.* **2004**, *279*, 20775–20785.

- (5) Iqbal, M.; Messina, P. A.; Freed, B.; Das, M.; Chatterjee, S.; Tripathy, R.; Tao, M.; Josef, K. A.; Dembofsky, B.; Dunn, D.; Griffith, E.; Siman, R.; Senadhi, S. E.; Biazzo, W.; Bozyczko-Coyne, D.; Meyer, S. L.; Ator, M. A.; Bihovsky, R. Subsite requirements for peptide aldehyde inhibitors of human calpain I. *Bioorg. Med. Chem. Lett.* **1997**, *7*, 539–544.
- (6) Moldoveanu, T.; Campbell, R. L.; Currier, D.; Davis, P. L. Crystal Structures of calpain-E64 and -leupeptin inhibitor complexes reveal mobile loops gating the active site. *J. Mol. Biol.* **2004**, *343*, 1313–1326.
- (7) Aoyagi, T.; Takeuchi, T.; Matsuzaki, A.; Kawamura, K.; Kondo, S. Leupeptines, new protease inhibitors from *Actinomyces*. *J. Antibiot.* **1969**, *22*, 283–286.
- (8) Sasaki, T.; Kishi, M.; Saito, M.; Tanaka, T.; Higuchi, N.; Kominami, N.; Katunuma, N.; Murachi, T. Inhibitory effect of di- and tripeptidyl aldehydes on calpains and cathepsins. *J. Enzyme Inhib.* **1990**, *3*, 195–201.
- (9) Mehdi, S. Cell-penetrating inhibitors of calpain. *Trends Biochem. Sci.* **1991**, *16*, 150–153.
- (10) Li, Z.; Ortega-Vilain, A.; Patil, G. S.; Chu, D.; Foreman, J. E. Novel peptidyl α -keto amide inhibitors of calpains and other cysteine proteases. *J. Med. Chem.* **1996**, *39*, 4089–4098.
- (11) Lubisch, W.; Beckenbach, E.; Bopp, S.; Hofmann, H. P.; Kartal, A.; Kästel, C.; Lindner, T.; Metz-Garrecht, M.; Reeb, J.; Regner, F.; Vierling, M.; Möller, A. Benzoylalanine-derived ketoamides carrying vinylbenzyl amino residues: Discovery of potent water-soluble calpain inhibitors with oral bioavailability. *J. Med. Chem.* **2003**, *46*, 2404–2412.
- (12) (a) Fukiage, C.; Azuma, M.; Nakamura, Y.; Tamada, Y.; Nakamura, M.; Shearer, T. R. SJA6017, A newly synthesized peptide aldehyde inhibitor of calpain: amelioration of cataract in cultured rat lenses. *Biochim. Biophys. Acta* **1997**, *1361*, 304–312. (b) Inoue, J.; Nakamura, M.; Cui, Y.; Sakai, Y.; Sakai, O.; Hill, J. R.; Wang, K. K. W.; Yuen, P.-W. Structure–activity relationship study and drug profile of *N*-(4-fluorophenylsulfonyl)-L-valyl-L-leucinal (SJA6017) as a potent calpain inhibitor. *J. Med. Chem.* **2003**, *46*, 868–871.
- (13) Lee, K. S.; Franks, S.; Vanderklisch, P.; Arai, A.; Lynch, G. Inhibition of proteolysis protects hippocampal neurons from ischemia. *Proc. Natl. Acad. Sci. U.S.A.* **1991**, *57*, 7233–7237.
- (14) Rami, A.; Kriegelstein, J. Protective effects of calpain inhibitors against neuronal damage caused by cytotoxic hypoxia and ischemia *in vivo*. *Brain Res.* **1993**, *609*, 67–70.
- (15) (a) Hong, S.-C.; Goto, Y.; Lanzino, G.; Saleau, S.; Kassel, N. F.; Lee, K. S. Neuroprotection with a calpain inhibitor in a model of focal cerebral ischemia. *Stroke* **1994**, *25*, 663–669. (b) Markgraf, C. G.; Velayo, N. L.; Johnson, M. P.; McCarty, D. R.; Medhi, S.; Koehl, J. R.; Chmielewski, P. A.; Linnik, M. D. Six-hour window of opportunity for calpain inhibition in focal cerebral ischemia in rats. *Stroke* **1998**, *29*, 152–158.
- (16) Bartus, R. T.; Hayward, N. J.; Elliott, P. J.; Sawyer, S. D.; Baker, K. L.; Dean, R. L.; Akiyama, A.; Straub, J. A.; Harbeson, S. L.; Li, Z.; Powers, J. Calpain inhibitor AK-295 protects neurons from focal brain damage. *Stroke* **1994**, *25*, 2265–2270.
- (17) Neuhof, W.; Götte, O.; Trumbeckaite, S.; Attenberger, M.; Kuzkaya, N.; Gellerish, F.; Möller, A.; Lubisch, W.; Speth, M.; Tillmanns, H.; Neuhof, H.; A novel water-soluble and cell-permeable calpain inhibitor protects myocardial and mitochondrial function in postischemic reperfusion. *Biol. Chem.* **2003**, *384*, 1597–1603.
- (18) Nath, R.; Davis, M.; Probert, A. W.; Kupina, N. C.; Ren, X.; Schielke, G. P.; Wang, K. K. Processing of cdk5 activator p35 to its truncated form (p25) by calpain in acutely injured neuronal cells. *Biochem. Biophys. Res. Commun.* **2000**, *274*, 16–21.
- (19) Sakamoto, Y.; Nakajima, T.; Fukiage, C.; Sakai, O.; Yoshida, Y.; Azuma, M.; Shearer, T. R. Involvement of calpain isoforms in ischemia-reperfusion injury in rat retina. *Curr. Eye Res.* **2000**, *21*, 571–580.
- (20) Sasaki, H.; Yamamura, K.; Mukai, T.; Nishida, K.; Nakamura, J.; Nakashima, M.; Ichikawa, M. Enhancement of ocular drug penetration. *Crit. Rev. Ther. Drug Carrier Syst.* **1999**, *16*, 85–146.
- (21) Sakamoto, Y. Unpublished results.
- (22) (a) Nakamura, M.; Inoue, J. Exploration of peptidyl hydrazones as water-soluble calpain inhibitors. *Bioorg. Med. Chem. Lett.* **2002**, *12*, 1603–1606. (b) Shirasaki, Y.; Miyashita, H.; Yamaguchi, M.; Inoue, J.; Nakamura, M. Exploration of orally available calpain inhibitors: peptidyl α -ketoamides containing an amphiphile at P3 site. *Bioorg. Med. Chem.* **2005**, *13*, 4473–4484.
- (23) Nakamura, M.; Yamaguchi, M.; Sakai, O.; Inoue, J. Exploration of cornea permeable calpain inhibitors as anticataract agents. *Bioorg. Med. Chem.* **2003**, *11*, 1371–1379.
- (24) Altmann, E.; Betschart, C.; Gohda, K.; Horiuchi, M.; Lattmann, R.; Missbach, M.; Sakaki, J.; Takai, M.; Teno, N.; Cowen, S. D.; Greenspan, P. D.; McQuire, L. W.; Tommasi, R. A.; Van D., John H. PCT Int. Appl. WO9924460, 1999.
- (25) (a) Angelastro, M. R.; Mehdi, S.; Burkhart, J. P.; Peet, N. P.; Bey, P. α -Diketone and α -keto ester derivatives of *N*-protected amino acids and peptides as novel inhibitors of cysteine and serine proteinases. *J. Med. Chem.* **1990**, *33*, 11–13. (b) Mehdi, S. Synthetic and naturally occurring protease inhibitors containing an electrophilic carbonyl group. *Bioorg. Chem.* **1993**, *21*, 249–259. (c) Otto, H.-H.; Schirmeister, T. Cysteine protease and their inhibitors. *Chem. Rev.* **1997**, *97*, 133–171. (d) Peet, N. P.; Kim, H. O.; Marquart, A. L.; Angelastro, M. R.; Nieduzak, T. R.; White, J. N.; Friedrich, D.; Flynn, G. A.; Webster, M. E.; Vaz, R. J.; Linnik, M. D.; Koehl, J. R.; Mehdi, S.; Bey, P.; Emary, B.; Hwang, K. K. Hydroxyoxazolidines as α -aminoacetaldehyde equivalents: novel inhibitors of calpain. *Bioorg. Med. Chem. Lett.* **1999**, *9*, 2365–2370.
- (26) Li, Z.; Patil, G. S.; Golubski, Z. E.; Hori, H.; Tehrani, K.; Foreman, J. E.; Eveleth, D. D.; Bartus, R. T.; Powers, J. C. Peptide α -keto ester, peptide α -keto amide and peptide α -keto acid inhibitors of calpains and other cysteine proteases. *J. Med. Chem.* **1993**, *36*, 3472–3480.
- (27) Nakamura, M.; Miyasita, H.; Yamaguchi, M.; Shirasaki, Y.; Nakamura, Y.; Inoue, J. Novel 6-hydroxy-3-morpholinones as cornea permeable inhibitors. *Bioorg. Med. Chem.* **2003**, *11*, 5449–5460.
- (28) van de Waterbeemd, H.; Smith, D. A.; Beaumont, K.; Walker, D. K. Property-based design: optimization of drug absorption and pharmacokinetics. *J. Med. Chem.* **2001**, *44*, 1313–1334.
- (29) Ando, R.; Sasaki, T.; Masuda, H.; Inakoshi, N.; Jikihara, T.; Fujimura, Y.; Niwa, T.; Yoshii, N.; Tabata, R. PCT Int. Appl. WO9625408, 1998.
- (30) Buroker-Kilgore, M.; Wang, K. K. W. A coomassie brilliant blue G-250-based colorimetric assay for measuring activity of calpain and other proteases. *Anal. Biochem.* **1993**, *208*, 387–392.

JM060157N